Chapter

Scalar Conservation Laws

Baver Okutmuştur

Abstract

We present a theoretical aspect of conservation laws by using simplest scalar models with essential properties. We start by rewriting the general scalar conservation law as a quasilinear partial differential equation and solve it by method of characteristics. Here we come across with the notion of strong and weak solutions depending on the initial value of the problem. Taking into account a special initial data for the left and right side of a discontinuity point, we get the related Riemann problem. An illustration of this problem is provided by some examples. In the remaining part of the chapter, we extend this analysis to the gas dynamics given in the Euler system of equations in one dimension. The transformations of this system into the Lagrangian coordinates follow by applying a suitable change of coordinates which is one of the main issues of this section. We next introduce a first-order Godunov finite volume scheme for scalar conservation laws which leads us to write Godunov schemes in both Eulerian and Lagrangian coordinates in one dimension where, in particular, the Lagrangian scheme is reformulated as a finite volume method. Finally, we end up the chapter by providing a comparison of Eulerian and Lagrangian approaches.

Keywords: conservation laws, Burgers' equation, shock and rarefaction waves, weak and strong solutions, Riemann problem, Euler system, Godunov schemes, Eulerian coordinates, Lagrangian coordinates

1. Introduction

We present a general form of scalar conservation laws with further properties including some basic models and provide examples of computational methods for them. The equations described by

$$\partial_t u + \partial_x f(u) = 0, \quad t > 0, x \in \mathbb{R} \tag{1}$$

in one dimension are known as scalar conservation laws where $u = u(t,x)$ is the conserved quantity and $f = f(u)$ is the associated flux function depending on t and x. Whenever an initial condition $u(0,x) = u_0(x)$ is attached to Eq. (1), the problem is called the Cauchy problem the solution of which is a content of this chapter. The outlook of chapter is as follows. We introduce basic concepts and provide particular examples of scalar conservation laws in the first part. The equation of gas dynamics in Eulerian coordinates in one dimension is the main issue

of the second part. After providing further instruction for these equations, we provide a transformation of the Eulerian equations in the Lagrangian coordinates. In the final part, we give as an example of computational methods for conservation laws, the Godunov schemes for the Eulerian, and the Lagrangian coordinates, respectively.

1.1 Conservation laws: integral form and differential form

We start by investigating the relation of the equations in gas dynamics with conservation laws. We take into account the equation of conservation of mass in one dimension. The density and the velocity are assumed to be constant in the tube where x is the distance and $\rho(t,x)$ is the density at the time t and at the point x. Then if we integrate the density on $[x_1,x_2]$, we get total mass $\int_{x_1}^{x_2}\rho(t,x)dx$ at time t. Assigning the velocity by $u(t,x)$, then mass flux at becomes $\rho(t,x)u(t,x)$. It follows that the rate of change of the mass in $[x_1,x_2]$ is

$$\frac{d}{dt}\int_{x_1}^{x_2}\rho(t,x)dx = \rho(t,x_1)u(t,x_1) - \rho(t,x_2)u(t,x_2). \tag{2}$$

The last equation is called integral form of conservation law. Integrating this expression in time from t_1 to t_2, we get

$$\int_{x_1}^{x_2}\rho(t_2,x)dx - \int_{x_1}^{x_2}\rho(t_1,x)dx = \int_{t_1}^{t_2}\rho(t,x_1)u(t,x_1)\,dt - \int_{t_1}^{t_2}\rho(t,x_2)u(t,x_2)\,dt. \tag{3}$$

Using the fundamental theorem of calculus after reduction of Eq. (3), it follows that

$$\rho(t,x_2)u(t,x_2) - \rho(t,x_1)u(t,x_1) = \int_{x_1}^{x_2}\partial_x(\rho(t,x)u(t,x))dx. \tag{4}$$

As a result, we get

$$\int_{t_1}^{t_2}\int_{x_1}^{x_2}\{\partial_t\rho(t,x) + \partial_x\rho(t,x)u(t,x)\}\,dx\,dt = 0. \tag{5}$$

Here the end points of the integrations are arbitrary; that is, for any $[x_1,x_2]$ and $[t_1,t_2]$, the integrant must be zero. It follows that the conservation of mass yields

$$\partial_t\rho + \partial_x(u\rho) = 0, \tag{6}$$

which is said to be the differential form of the conservation law.

1.2 A first-order quasilinear partial differential equations

A general solution to a quasilinear partial differential equation of the form

$$a(t,x,u)\partial_t u + b(t,x,u)\partial_x u = c(t,x,u) \tag{7}$$

where a,b,c are non-zero and smooth on a given domain $D\in\mathbb{R}^3$ follows by the characteristic method where the characteristic curves are defined by

$$\frac{dt}{a(t,x,u)} = \frac{dx}{b(t,x,u)} = \frac{du}{c(t,x,u)}. \tag{8}$$

By applying a parametrization of c, the relation (8) is transformed to a system of ordinary differential equation (ODE):

$$\frac{dt}{dc} = a(t,x,u), \quad \frac{dx}{dc} = b(t,x,u), \quad \frac{du}{dc} = c(t,x,u). \tag{9}$$

In addition to these equations, if an initial condition $u_0 = u(x_0)$ is also given, then by the existence theorem of ODE, there is a unique characteristic curve passing from each point (t_0, x_0, u_0) leading to an integral surface which is the solution to Eq. (7).

Observe that the scalar conservation law (1) is a particular example of Eq. (7) if we assign $a(t,x,u) = 1$, $b(t,x,u)u_x = (f(u))_x$, and $c(t,x,u) = 0$. The conserved quantity can be observed by integrating equation (1) over $[x_0, x_1]$. Indeed

$$\begin{aligned} \frac{d}{dt}\int_{x_0}^{x_1} u(t,x)\,dx &= \int_{x_0}^{x_1} \partial_t u(t,x)\,dx = -\int_{x_0}^{x_1} f(u(t,x))_x\,dx \\ &= f(u(t,x_1)) - f(u(t,x_0)) \\ &= [\text{inflow at the point } x_1] - [\text{outflow at the point } x_0]. \end{aligned} \tag{10}$$

This means, the quantity $u(t,x)$ is conserved so that it depends on the difference of the flux functions between the points x_0 and x_1.

1.3 Strong (classical) solutions

We consider the initial value problem

$$\begin{aligned} &\partial_t u + \partial_x(f(u)) = 0, \quad t > 0, \quad x \in \mathbb{R} \\ &u(0,x) = u_0(x), \quad x \in \mathbb{R} \end{aligned} \tag{11}$$

where the initial data is assumed to be continuously differentiable, that is, $u_0(x) \in C^1(\mathbb{R})$. Applying the chain rule to the relation (11), it follows that

$$\begin{aligned} &\partial_t u + f'(u)\,\partial_x u = 0, \quad t > 0, \quad x \in \mathbb{R}, \\ &u(0,x) = u_0(x), \quad x \in \mathbb{R}, \end{aligned} \tag{12}$$

where we define characteristic curves of Eq. (12) to be the solution of $\frac{d}{dt}x(t) = f'(u(t,x(t))) = f'(u)$. Then a solution to the system (12) in a domain $\Omega \in \mathbb{R}$ is said to be a strong (or classical) solution if it satisfies Eq. (11), and it is continuously differentiable on a domain $\Omega \in \mathbb{R}$. Let u be a strong solution and the initial data u_0 be differentiable. Observe that (12) is equivalent to a quasilinear form:

$$\partial_t u + \lambda(u)\partial_x u = 0, \tag{13}$$

with $\lambda(u) = f'(u)$. Applying the method of characteristics to Eq. (13), the partial differential equation is transformed to a system of ordinary differential equations. We consider the characteristic curve passing through the point $(0, x_0)$:

$$\begin{aligned} \partial_t x &= \lambda(u(t,x(t))) \\ x(0) &= x_0. \end{aligned} \tag{14}$$

Along this characteristic curve,

$$\partial_t u(t,x(t)) = \partial_t u(t,x(t)) + \partial_t x \partial_x u(t,x(t)) = \partial_t u + \lambda(u)\partial_x u = 0 \tag{15}$$

is satisfied, that is, u is constant. Hence, the characteristic curves are straight lines satisfying

$$x = x_0 + \lambda(u_0(x_0))t = 0. \tag{16}$$

Hence we can define smooth solutions by $u(t,x) = u_0(x_0)$. If the slope of the characteristics is $m_{char} = \frac{1}{\lambda(u_0(x_i))}$, then depending on the behavior of λ, the solution takes different forms. If $\lambda(u_0(x))$ is increasing, then the slopes of the characteristics are decreasing. As a result, the characteristics do not intersect, and thus solution can be defined for all t which is greater than zero. On the other hand, if $\lambda(u_0(x))$ is decreasing, then the slopes of the characteristics will be increasing which implies that the characteristics intersect at some point. But at the intersection point, solution cannot take both values $u_0(x_1)$ and $u_0(x_2)$. Therefore, we cannot define the strong solution for all $t > 0$.

1.4 Linear advection equation

The basic example of the scalar conservation law is the linear advection equation. It can be obtained by setting $a(t,x,u) = 1$, $b(t,x,u) = \lambda$, and $c(t,x,u) = 0$ in Eq. (7). The flux function takes the form $f(u) = \lambda u$ where λ is a constant. Then the following quasilinear partial differential equation

$$\partial_t u + \lambda \partial_x u = 0 \tag{17}$$

is a linear advection equation. Similar to Eqs. (11) and (12), an initial value problem for linear advection equation is described by

$$\begin{aligned} &\partial_t u + \partial_x f(u) = 0, \quad -\infty < x < \infty, \quad t \geq 0, \\ &u(0,x) = u_0(x) = f(x_0), \quad -\infty < x < \infty. \end{aligned} \tag{18}$$

Applying the method of characteristics, it follows that $\frac{dt}{1} = \frac{dx}{\lambda} = \frac{du}{0}$ or equivalently

$$u = c_1, \quad \frac{dx}{dt} = \lambda = c_1, \quad x = c_1 t + c_2, \tag{19}$$

where c_1 and c_2 are constant and $x - \lambda t = c_2$. As a conclusion, the solution is

$$u(t,x) = u_0(x - \lambda t), \quad t \geq 0. \tag{20}$$

Here λ is the wave speed, and the characteristic lines $x - \lambda t = c_2$ are wavefronts which are constants.

1.5 Burgers' equation

Burgers' equation is the simplest nonlinear partial differential equation and is the one of the most common models used in the scalar conservation laws and fluid dynamics. The classical Burgers' equation is described by

$$\partial_t u + u\partial_x u = \nu \partial_{xx} u, \tag{21}$$

where $\nu\partial_{xx}u$ is the viscosity term. Equation (21) can be considered as a combination of nonlinear wave motion and linear diffusion term so that it is balance between time evolution, nonlinearity, and diffusion. The term $u\partial_x u$ is a convection term that may have an effect to wave breaking, and the term $\nu\partial_{xx}u$ is a diffusion term that may cause to efface the wave breaking and to flatten discontinuities, and thus we expect to achieve a smooth solution. We try to find a traveling wave solution of Eq. (21) of the form

$$u(t,x) = g(\xi) = g(x - \lambda t), \quad \text{with} \quad \xi = x - \lambda t, \tag{22}$$

where g and λ are to be determined. Applying the chain rule, we get

$$\partial_t u = -\lambda g'(\xi), \quad \partial_x u = g'(\xi), \quad \partial_{xx} u = g''(\xi). \tag{23}$$

Plugging these terms in Eq. (21), we get

$$-\lambda g'(\xi) + g(\xi)g'(\xi) - \nu g''(\xi) = 0. \tag{24}$$

Taking integration with respect to ξ gives

$$-\lambda g + \frac{1}{2}g^2 - \nu g' = C, \quad C : \textit{constant}. \tag{25}$$

Rewriting Eq. (25) by

$$(g - g_1)(g - g_2) = g^2 - 2\lambda g - 2C = 2\nu\, dg/d\xi, \tag{26}$$

it follows that $g_{1,2} = \lambda \pm \sqrt{\lambda^2 + 2C}$. Supposing that g_1,g_2 are real implies $g_1 > g_2$. Using separation of variable and then integrating equation (26), we get

$$g(\xi) = \frac{g_1 + g_2 e^{\left(\frac{g_1 - g_2}{2\nu}\right)\xi}}{1 + e^{\left(\frac{g_1 - g_2}{2\nu}\right)\xi}} = \frac{g_1 + g_2}{2} - \frac{g_1 - g_2}{2}\tan h\left(\frac{g_1 - g_2}{4\nu}\xi\right) \tag{27}$$

As a result the explicit form of traveling wave solution of Eq. (21) becomes

$$u(t,x) = \lambda - \frac{g_1 - g_2}{2}\tan h\left(\frac{1}{4\nu}(g_1 - g_2)(x - \lambda t)\right) \tag{28}$$

where $\lambda = \frac{g_1 + g_2}{2}$ is the wave speed. We can observe that $\lim_{\xi \to -\infty} g(\xi) = g_1$ and $\lim_{\xi \to \infty} g(\xi) = g_2$ with $g'(\xi) < 0$ for all ξ. This means the solution $g(\xi)$ decreases monotonically with ξ from the value g_1 to g_2. At $\xi = 0, u = \frac{g_1 + g_2}{2} = \lambda,$ that is the wave form $g(\xi)$ travels from left to right with speed λ equal to the average value of its asymptotic values. The solution resembles to a shock form as it connects the asymptotic states g_1 and g_2. Without the viscosity term, the solutions to Burgers equation allow shock forms which finally break. The diffusion term prevents incrementally deformation of the wave and its breaking by withstanding the nonlinearity. As a conclusion, there exists a balance between nonlinear advection term and the linear diffusion term. The wave form is notably affected by the diffusion coefficient ν. If ν is smaller, then the transition layer between two asymptotic values of solution is sharper. In the limit $\nu \to 0$, the solutions converge to the step shock wave solutions to the inviscid Burgers' equation.

Remark. If the initial data is smooth and very small, then the u_{xx} term is negligible compared to other terms before the beginning of wave breaking. As the wave breaking starts, the u_{xx} term raises faster than u_x term. After a while, the term u_{xx} becomes comparable to the other terms so that it keeps the solution smooth, giving rise to avoid breakdown solutions.

1.6 Inviscid Burgers' equation

Whenever $\nu = 0$, Eq. (21) is called the inviscid Burgers' equation. This equation can be obtained by substituting $f(u) = u^2/2$ in the scalar conservation law (1), that is

$$\partial_t u + \partial_x\left(u^2/2\right) = \partial_t u + u\partial_x u = 0. \tag{29}$$

Observe that $f(u)$ is a nonlinear function of u; thus, the inviscid Burgers' equation is a nonlinear equation. Equation (29) is now equivalent to Eq. (17) with $\lambda = u$. We know the solution of Eq. (17); so, plugging $\lambda = u$ into the relation (20) implies that the solution of Eq. (29) is

$$u(t,x) = f(x - ut) = u_0(x - ut). \tag{30}$$

Recall that the characteristic speed λ is constant for linear advection equation; that is, the characteristic curves become parallel for Eq. (17). In contrast, for the inviscid Burgers' equation (29), the characteristic speed $\lambda = u$ depends on u. As a result the characteristic lines are not parallel. If we apply the implicit function theorem to Eq. (29), the solution can be written as a function of t and x as u_0 is differentiable. More particularly, differentiating Eq. (30) with respect to t, we get

$$\partial_t u = -u_0'(u_t t + u) \quad \Rightarrow \partial_t u = -\frac{u_0' u}{1 + u_0' t}; \tag{31}$$

and differentiating equation (30) with respect to x, we get

$$\partial_x u = u_0'(1 - u_x t) \quad \Rightarrow \partial_x u = \frac{u_0'}{1 + u_0' t}. \tag{32}$$

Thus, substituting Eqs. (31) and (32) in (29), we can recover the inviscid Burgers' equation. Consequently, the relations (31) and (32) imply that the solutions of Eq. (1) and particularly of Eq. (29) depend on the initial value u_0. It can be observed that whenever $u_0'(x) > 0$, then by Eq. (32), $\partial_x u$ decreases in time because $1 + u_{0'} t > 0$ for $t > 0$. In other words, the profile of the wave flattens as time increases. On the other hand, whenever $u_0'(x) < 0$, then $\partial_x u$ increases in time as $1 + u_0 t < 0$. Hence u_x in Eq. (32) tends to ∞ as $1 + u_0' t$ approaches to zero. As a result, wave profile become sharp after some time. For further details on the Burgers' equations, we refer the reader to [12, 13, 22] and the references therein.

1.7 Shock waves

Let the constants u_L and u_R are given with a linear function, $\varphi(t) = \lambda t$. Then

$$u(t,x) = \begin{cases} u_R & \text{if} \quad x > \lambda t, \\ u_L & \text{if} \quad x < \lambda t, \end{cases} \tag{33}$$

is a simple example of discontinuous solution of the conservation law (11). If $u_L \neq u_R$, the relation (33) is called a shock wave connecting u_L to u_R with shock speed λ. As an example, if we take into account the characteristics of the inviscid Burgers' equations which are of the form $\frac{dx}{dt} = u(t,x)$, it follows that

$$x(t) = u_0(x_0)t + x_0 \tag{34}$$

where $u_0(x) = u(0,x)$ and $x_0 = x(0)$; thus, the characteristics are straight lines. Depending on the behavior of these characteristics, we have two cases. If $u_L > u_R$, characteristics intersect, the solution will have an infinite slope, and the wave will break; as a result a shock is obtained. This is illustrated in **Figure 1**. On the other hand, if $u_R > u_L$, the characteristics do not intersect, and hence a region without characteristic will appear which is physically unacceptable. This is shown in **Figure 2**. We get rid of this by introducing the rarefaction waves.

1.8 Rarefaction waves

A rarefaction wave is a strong solution which is a union of characteristic lines. A rarefaction fan is a collection of rarefaction waves. These waves are constant on the characteristic line $x - x_0 = \alpha t$. Here $\alpha \in \left(f'(u_L), f'(u_R)\right)$ where u_L and u_R are the values of u at the edge of the rarefaction wave fan. If moreover f' is invertible, then the solution $u = u(t,x)$ satisfies

$$u(x,t) = \left(f'\right)^{-1}\left(\frac{x - x_0}{t}\right). \tag{35}$$

If, for instance, f is convex, then the rarefaction waves are increasing. If we consider again the inviscid Burgers' equation with the initial values, then the region without characteristics in **Figure 2** will be covered by rarefaction solution which is described by

$$u(t,x) = \begin{cases} u_L & \text{if} \quad x/t \leq f'(u_L), \\ \left(f'\right)^{-1}(x/t) & \text{if} \quad f'(u_L) \leq x/t \leq f'(u_R), \\ u_R & \text{if} \quad f'(u_R) \leq x/t. \end{cases} \tag{36}$$

Figure 1.
For the initial value $u_L > u_R$, characteristics, and shock wave.

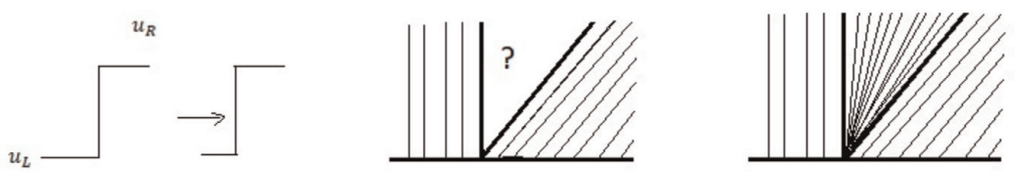

Figure 2.
For the initial value $u_R > u_L$, characteristics and rarefaction waves.

An illustration of rarefaction waves and rarefaction fan in Eq. (36) is given in **Figure 3**.

Remark. Whenever characteristics intersect, we may have multiple valued solution or no solution; but we have no more classical (strong) solution. To get rid of this situation, we introduce a more wide-ranging notion of solution, the weak solution, in the next part. By this arrangement, we may have non-differentiable and even discontinuous solutions.

1.9 Weak solution

Weak solutions occur whenever there is no smooth (classical) solution. These solutions may not be differentiable or even not continuous. Considering $\phi : \mathbb{R} \times \mathbb{R}^+ \to \mathbb{R}$ as a smooth test function with a compact support and multiplying the scalar conservation law (1) by this test function ϕ, it follows after integration by parts that

$$\begin{aligned}
&\int_0^\infty \int_{-\infty}^\infty \phi \partial_t u + \phi \partial_x f(u)\, dx\, dt \\
&= \int_{-\infty}^\infty \phi u \Big|_0^\infty dx - \int_0^\infty \int_{-\infty}^\infty u \partial_t \phi\, dx\, dt + \int_0^\infty \phi f(u) \Big|_{-\infty}^\infty dt - \int_0^\infty \int_{-\infty}^\infty f(u)\, \partial_x \phi\, dx\, dt \\
&= -\int_0^\infty \int_{-\infty}^\infty u \partial_t \phi\, dx\, dt - \int_0^\infty \int_{-\infty}^\infty f(u)\, \partial_x \phi\, dx\, dt - \int_{-\infty}^\infty u\phi \Big|_{t=0} dx.
\end{aligned} \tag{37}$$

Putting the initial condition $u_0(x) = u(0,x)$ to the above relation, it follows that

$$\int_0^\infty \int_{-\infty}^\infty u\phi_t + f(u)\phi_x dx\, dt + \int_{-\infty}^\infty u(0,x)\phi(x) dx = 0. \tag{38}$$

Observe that there are no more derivatives of u and f which may lead less smoothness. In other words, the smoothness requirement is reduced for finding a solution. Thus, the function $u(t,x)$ is said to be the weak solution of the initial value problem (11) if the relation (38) satisfied for all test function ϕ. Here it is significant to note that u needs not be smooth or continuous to satisfy Eq. (38). Consequently, by weak solutions, we extend the solutions so that discontinuous solutions may also be covered. However, in general weak solutions are not unique. We can also notice

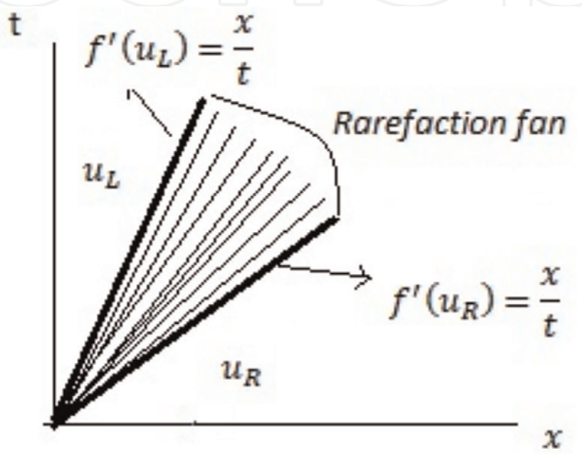

Figure 3.
Rarefaction fan.

that strong solutions are also weak solutions and a weak solution which is continuous and piecewise differentiable is also strong solution.

1.10 Riemann problem

The Riemann problem is a Cauchy problem with a particular initial value which consists a conservation law together with piecewise constant data having a single discontinuity. We consider the Riemann problem for a convex flux described by

$$\begin{aligned} &\partial_t u + \partial_x(f(u)) = 0, \quad x \in \mathbb{R}, \quad t \in \mathbb{R}_+, \\ &u(0,x) = \begin{cases} u_L & \text{if} \quad x < 0, \\ u_R & \text{if} \quad x > 0. \end{cases} \end{aligned} \tag{39}$$

The solution is a set of shock and rarefaction waves depending on the relation between u_L and u_R. There are two cases to investigate:

Case 1: $(u_L > u_R)$ A shock is obtained because the left-hand side wave moves faster than the right-hand side one. Thus the solution

$$u(t,x) = \begin{cases} u_L & \text{if} \quad x/t < \lambda, \\ u_R & \text{if} \quad x/t > \lambda, \end{cases} \tag{40}$$

is a shock wave satisfying the shock speed $\lambda = \frac{f(u_R) - f(u_L)}{u_R - u_L}$.

Case 2: $(u_L < u_R)$ The solution given in Case 1 is also a solution for this case. In addition, we have rarefaction solutions of the form (36) illustrated by **Figure 3**.

1.11 Rankine-Hugoniot jump condition

A jump discontinuity along the characteristic line is controlled by the Rankine-Hugoniot jump condition. Integrating the scalar conservation law (1) in $[x_1, x_2]$, it follows that

$$\frac{d}{dt}\int_{x_1}^{x_2} u(t,x)dx + f(u)\Big|_{x_1}^{x_2} = 0. \tag{41}$$

Suppose that there is a discontinuity at the point $x = \xi(t) \in (x_1, x_2)$ where u and u' are continuous on the $[x_1, \xi(t))$ and $(\xi(t), x_2]$, respectively. Suppose also that whenever $x_1 \to \xi(t)^-$ and $x_2 \to \xi(t)^+$, their limits exist. Next, Eq. (41) can be rewritten as

$$\frac{d}{dt}\int_{x_1}^{\xi(t)} u(t,x)dx + \frac{d}{dt}\int_{\xi(t)}^{x_2} u(t,x)dx = -(f(t,x_2) - f(t,x_1)). \tag{42}$$

By the fundamental theorem of calculus, the relations (41) and (42) yield

$$u(\xi^-,x)\xi'(t) - u(\xi^+,x)\xi'(t) + \frac{d}{dt}\int_{x_1}^{\xi(t)} u_t(t,x)dx + \frac{d}{dt}\int_{\xi(t)}^{x_2} u_t(t,x)dx. \tag{43}$$

Taking the limit whenever $x_1 \to \xi(t)^-$ and $x_2 \to \xi(t)^+$, it follows that

$$\xi'(t)(x_2 - x_1) = f(x_2) - f(x_1) \Rightarrow \lambda = \xi'(t) = \frac{f(x_2) - f(x_1)}{x_2 - x_1}. \tag{44}$$

The relation (44) is said to be the Rankine-Hugoniot jump condition. Geometrical meaning of the Rankine-Hugoniot jump condition is that the shock speed is the slope of the secant line through the points $(u_L, f(u_L))$ and $(u_R, f(u_R))$ on the graph of f.

1.12 Entropy functions

Entropy and entropy flux are defined for attaining physically meaningful solutions. If u is the smooth solution of the conservation law (1), then the relation

$$\partial_t G(u) + \partial_x F(u) = 0 \tag{45}$$

is satisfied for continuously differentiable functions G and F where the pair (G, F) is called as entropy pair so that G is entropy and F is entropy flux. If in addition u is smooth, then Eq. (45) becomes

$$G'(u)\partial_t u + F'(u)\partial_x u = 0 \tag{46}$$

which looks like to the scalar conservation law (1). Indeed, if we multiply Eq. (1) by $G'(u)$, it follows that

$$G'(u)\partial_t u + G'(u)f'(u)\partial_x u = 0. \tag{47}$$

It follows that Eqs. (46) and (47) are equivalent with $F'(u) = G'(u)f'(u)$. Here the function $u(t, x)$ is said to be the entropy solution of Eq. (1) if

$$\partial_t G(u) + \partial_x F(u) \leq 0$$

holds for all convex entropy pairs $(G(u), F(u))$.

1.13 Entropy condition

Weak solutions to conservation laws may contain discontinuities as a result of a discontinuity in the initial data or of characteristics that cross each other or because of the jump conditions which are satisfied across the discontinuities. Although the Rankine-Hugoniot jump condition is satisfied, the uniqueness of the solution may always not be guaranteed. In order to eliminate the nonphysical solutions among the weak solutions, we need an additional condition, so-called entropy condition. It is described by the following: A discontinuity propagating with the characteristic speed λ given by the Rankine-Hugoniot jump condition satisfies the entropy condition if holds.

$$f'(u_L) > \lambda > f'(u_R) \tag{48}$$

Example 1.1. The weak solutions to conservation laws need not be unique. If we write the inviscid Burgers' equation in quasilinear form and multiply by $2u$, we obtain $2u\partial_t u + 2u^2\partial_x u = 0$. In conservative form it becomes

$$\partial_t\left(u^2\right) + \partial_x\left(\frac{2}{3}u^3\right) = 0, \quad \text{with } f\left(u^2\right) = \frac{2}{3}\left(u^2\right)^{3/2}. \tag{49}$$

The inviscid Burgers' equation and Eq. (49) have exactly the same smooth solutions. But their weak solutions are different. A shock traveling speed for the

inviscid Burgers' equation is $\lambda_1 = (u_L + u_R)/2$; however for Eq. (49), we have $\lambda_2 = \left(\frac{2}{3}\left(\frac{u_L^3 - u_R^3}{u_L^2 - u_R^2}\right)\right)$. That is $\lambda_1 \neq \lambda_2$ whenever $u_L \neq u_R$, and thus these two equations have different weak solutions.

Example 1.2. We first consider the initial value problem for $u_L > u_R$ given by

$$\partial_t u + \partial_x\left(u^2/2\right) = 0, \quad u_0 = \begin{cases} 1 & \text{if} \quad x \leq 0, \\ 0 & \text{if} \quad x > 0. \end{cases} \tag{50}$$

Applying the method of characteristics for $t > 0$, it follows that

$$\frac{du}{dt} = 0, \quad \frac{dx}{dt} = \begin{cases} 1 & \text{if} \quad x \leq 0, \\ 0 & \text{if} \quad x > 0. \end{cases} \tag{51}$$

Next if we integrate Eq. (51) with respect to t, we get the characteristic curves

$$x = \begin{cases} t - c & \text{if} \quad x \leq 0, \\ b & \text{if} \quad x > 0, \end{cases} \tag{52}$$

where $c > 0$ and b are constants. Due to the discontinuity at the point $x = 0$, there is no strong (classical) solution. The speed of propagation is $\lambda = \frac{u_L + u_R}{2} = 0.5$. Moreover, the weak solution for $t \leq \lambda = 0.5$ becomes

$$u(t,x) = \begin{cases} 1 & \text{if} \quad \dfrac{x}{t} \leq 0.5 \\ 0 & \text{if} \quad \dfrac{x}{t} > 0.5 \end{cases}, \tag{53}$$

which satisfies both the jump condition and the entropy condition as $u_L = 1 > u_R = 0$. The characteristic curves can be observed in **Figure 4**.

Example 1.3. We now interchange the roles of u_L and u_R of the Example 1.2 so that $u_L < u_R$ to get an initial value problem:

$$\partial_t u + \partial_x\left(u^2/2\right) = 0, \quad u_0 = \begin{cases} 0 & \text{if} \quad x \leq 0, \\ 1 & \text{if} \quad x > 0. \end{cases} \tag{54}$$

By the method of characteristics, we obtain a solution

$$u_1(t,x) = \begin{cases} 0 & \text{if} \quad \dfrac{x}{t} \leq 1 \\ 1 & \text{if} \quad \dfrac{x}{t} > 1 \end{cases} \tag{55}$$

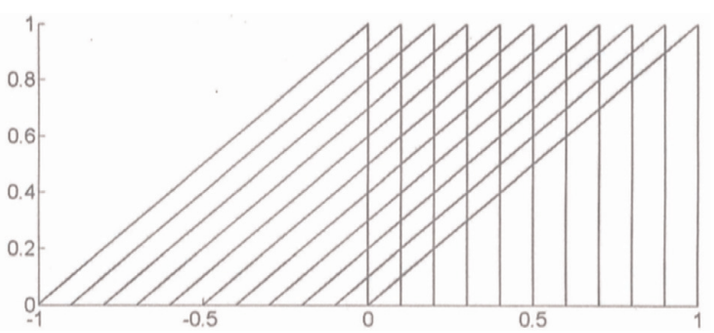

Figure 4.
For initial value $u_L > u_R$, the characteristic solutions.

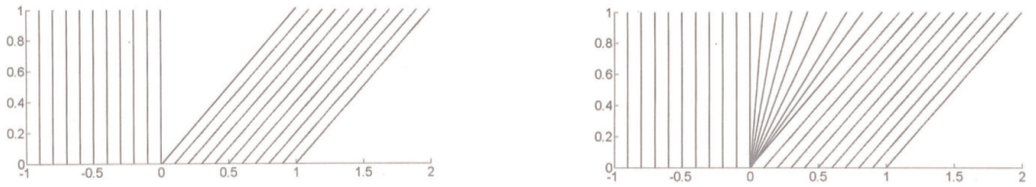

Figure 5.
For initial value $u_L < u_R$, characteristic solutions $u_1(t,x)$ and $u_2(x,t)$ with rarefaction fan.

which is a classical (strong) solution on both sides of the characteristic line $\frac{x}{t} = 1$. Since it satisfies the Rankine-Hugoniot jump condition along the discontinuity curve, it is a weak solution. However, the entropy condition is not satisfied. It yields an empty region between the characteristic lines shown in **Figure 4**. In order to cover this empty state, we consider another solution described by

$$u_2(t,x) = \begin{cases} 0 & \text{if} \quad x \le 0, \\ \dfrac{x}{t} & \text{if} \quad 0 \le \dfrac{x}{t} \le 1, \\ 1 & \text{if} \quad \dfrac{x}{t} \ge 1 \end{cases} \tag{56}$$

which satisfies both jump and entropy conditions. Here we can observe the rarefaction fan arising on the interval $0 \le \frac{x}{t} \le 1$. An illustration of this solution is supplied in **Figure 5**.

2. The gas dynamic equations in one dimension

The equation of fluid dynamics can be represented in Eulerian and Lagrangian forms. Eulerian coordinates are related to the coordinates of a fixed observer. On the other hand, Lagrangian coordinates are in usual related to the local flow velocity. That is, due to the velocity taking different values in different parts of the fluid, the change of coordinates is different from one point to another one.

2.1 Eulerian coordinates

The equations of gas dynamics in Eulerian coordinates can be written in the following conservative forms:

$$\begin{cases} \partial_t(\rho) + \partial_x(\rho u) = 0, \\ \partial_t(\rho u) + \partial_x(\rho u^2 + p) = 0, \\ \partial_t(\rho e) + \partial_x((\rho e + p)u) = 0 \end{cases} \tag{57}$$

where we ignored the heat conduction. If we denote

$$U = \begin{pmatrix} \rho \\ \rho u \\ \rho e \end{pmatrix}, \quad F(U) = \begin{pmatrix} \rho e \\ \rho u^2 + p \\ \rho e u + p u \end{pmatrix}, \tag{58}$$

then Eq. (57) can be written by

$$\partial_t U + \partial_x F(U) = 0 \tag{59}$$

where ρ is density, p is pressure, u is velocity, and e is the specific internal energy.

2.2 Hyperbolicity of the Euler system

If we do not neglect the heat conduction, then the U and F terms in Eq. (59) become

$$U = \begin{pmatrix} \rho \\ \rho u \\ E \end{pmatrix} \quad \text{and} \quad F = \begin{pmatrix} \rho u \\ \rho u^2 + p \\ (E+p)u \end{pmatrix}, \tag{60}$$

where E is total energy such that $E = \frac{1}{2}\rho u^2 + \rho e,\ e = \frac{p}{(\delta-1)\rho}$, and for perfect gases $\delta = c_p/c_v$ is the ratio of specific heats. Rewriting Eq. (59) in quasilinear form, we get

$$\partial_t U + A(U)\partial_x U = 0, \tag{61}$$

where $A(U) = \frac{\partial F}{\partial U}$ is the Jacobian matrix. The eigenvalues of $A(U)$ then are $\lambda_1 = u, \quad \lambda_2 = u - a, \quad \lambda_3 = u + a$ where a is the sound speed given by $a = \sqrt{\frac{\delta p}{\rho}}$. Moreover the corresponding eigenvectors are

$$E^{(1)} = \begin{pmatrix} 1 \\ u \\ \frac{1}{2}u^2 \end{pmatrix}, \quad E^{(2)} = \begin{pmatrix} 1 \\ u - a \\ H - ua \end{pmatrix}, \quad E^{(3)} = \begin{pmatrix} 1 \\ u + a \\ H + ua \end{pmatrix} \tag{62}$$

which are real, and the eigenvectors are linearly independent implying that the Euler equations for perfect gases are hyperbolic.

2.3 Rankine-Hugoniot conditions for the Euler system

Using the results in the previous part, the Rankine-Hugoniot jump conditions for the Euler system will be of the form

$$\begin{aligned} s(\rho_1 - \rho_2) &= m_2 - m_1, \\ s(m_2 - m_1) &= \frac{m_2^2}{\rho_2} + p_2 - \frac{m_1^2}{\rho_1} - p_1, \\ s(\rho_2 E_2 - \rho_1 E_1) &= m_2 H_2 - H_1 m_1, \end{aligned} \tag{63}$$

where the indices 1 and 2 refer to the left and right of the shock, respectively, and s denotes the wave speed.

2.4 Riemann problem for the Euler system

The Riemann problem for the one-dimensional Euler equation (57) is represented by

$$\begin{aligned} &\partial_t U + \partial_x(F(U)) = 0, \quad x \in \mathbb{R}, \quad t > 0, \\ &U(0,x) = U_0(x) = \begin{cases} U_L & \text{if} \quad x < 0, \\ U_R & \text{if} \quad x > 0. \end{cases} \end{aligned} \tag{64}$$

The reader is addressed to the references [18, 24] for further details.

2.5 Lagrangian coordinates

We aim to transform the equations of gas dynamics (57) given in the Eulerian coordinates into the Lagrangian coordinates for one-dimensional case. We start denoting by $\mathbf{u} = \mathbf{u}(t,x)$ the velocity field of the fluid flow and consider the differential system

$$\frac{dx}{dt} = \mathbf{u}(t,x). \tag{65}$$

We set the following change of coordinates from Euler coordinates to Lagrange coordinates for space and time as $(t,x) \to (t',\xi)$ where $\xi = (\xi_1,\xi_2,\xi_3) \in \mathbb{R}^3$ so that

$$t' = t, \quad \frac{\partial x(t',\xi)}{\partial t'} = \mathbf{u}(t',x(t',\xi)), \quad x_0 = x(0,\xi) = \xi. \tag{66}$$

It follows that $(t',\xi) = (t,(\xi_1,\xi_2,\xi_3))$ are the Lagrangian coordinates associated with the velocity field u. We set

$$J(t,\xi) = \det\left(\frac{\partial x_i}{\partial \xi_j}(t,\xi)\right), \tag{67}$$

which gives

$$\frac{\partial J}{\partial t}(t,\xi) = J(t,\xi)(\mathbf{div}\,\mathbf{u})(t,x(t,\xi)), \qquad \text{where,} \qquad \mathbf{div}\,\mathbf{u} = \sum_{j=1}^{3}\frac{\partial u_j}{\partial x_j}. \tag{68}$$

It follows by some algebraic manipulations that the gas dynamic equations become

$$\begin{cases} \partial_t(\rho J) = 0, \quad (\text{Conservation of mass}), \\ \partial_t(\rho u J) + \partial_\xi(p) = 0, \quad (\text{Conservation of momentum}), \\ \partial_t(\rho e J) + \partial_\xi(pu) = 0, \quad (\text{Conservation of energy}). \end{cases} \tag{69}$$

In order to derive a more convenient form of the system (69), we derive firstly the equation of conservation of mass:

$$\rho J = \rho_0 = \rho(0,\xi) \tag{70}$$

where $\rho_0(\xi) = \rho(0,\xi)$. Assuming that $\rho > 0$, we introduce the specific volume $\tau = 1/\rho$, and by using Eq. (68) we get

$$J = \rho_0\tau, \quad \text{and} \quad \partial_t J = J\partial_x u = \partial_\xi u \tag{71}$$

which yields

$$\rho_0\partial_t\tau - \partial_\xi u = 0. \tag{72}$$

Hence the second and third equations of Eq. (69) become

$$\begin{aligned} &\rho_0\partial_t u + \partial_\xi p = 0, \quad (\text{Conservation of momentum}), \\ &\rho_0\partial_t e + \partial_\xi(pu) = 0, \quad (\text{Conservation of energy}). \end{aligned} \tag{73}$$

Moreover, we define a mass variable m by

$$m(\xi) = \int_0^{\xi} \rho(0,y)dy, \quad \text{or equivalently,} \quad dm = \rho(0,\xi)d\xi = \rho_0 d\xi. \tag{74}$$

Finally, using Eqs. (69) and (73), the Euler system (57) can be written in Lagrangian coordinates with the mass variable in the form

$$\begin{cases} \partial_t \tau - \partial_m u = 0, \\ \partial_t u + \partial_m p = 0, \\ \partial_t e + \partial_m (pu) = 0, \end{cases} \tag{75}$$

where $p = p(\tau,\xi) = p(\tau, e - u^2/2)$. If we set $V = \begin{pmatrix} \tau \\ u \\ e \end{pmatrix}$, $F(V) = \begin{pmatrix} -u \\ p \\ pu \end{pmatrix}$ with $\tau > 0, u \in \mathbb{R}, e - u^2/2 > 0,$ we obtain a scalar conservation law of the form

$$\partial_t V + \partial_m F(V) = 0 \tag{76}$$

which is strictly hyperbolic. This can be verified by checking the Jacobian matrix of the flux calculated with respect to the variables (τ, u, e)

$$\begin{pmatrix} 0 & -1 & 0 \\ p_\tau & -up_\varepsilon & p_\varepsilon \\ up_\tau & p - u^2 p_\varepsilon & up_\varepsilon \end{pmatrix} \tag{77}$$

with $e = \varepsilon + \frac{1}{2}u^2$. The eigenvalues are $\sigma_1 = -\sqrt{p_\tau - pp_\varepsilon} < \sigma_2 = 0 < \sigma_3 = \sqrt{p_\tau - pp_\varepsilon}$ so that they are all distinct, and thus the system is strictly hyperbolic.

In fact there are different versions of the gas dynamics in Lagrangian coordinates. In this part we followed the approaches stated in [9, 10, 12]. For further details we cite these works with references therein.

2.6 Rankine-Hugoniot conditions for the Lagrangian system

Similarly as in the Euler system, the Rankine-Hugoniot jump conditions for the Lagrangian system (79) are of the form

$$\begin{aligned} &\sigma(\tau_1 - \tau_0) = -(u_1 - u_0), \\ &\sigma(u_1 - u_0) = p_1 - p_0, \\ &\sigma(e_1 - e_0) = p_1 u_1 - p_0 u_0, \end{aligned} \tag{78}$$

where σ denotes the speed of propagation of the discontinuity with respect to the mass variable.

Remark. The Eulerian and Lagrangian Rankine-Hugoniot relations are equivalent. Moreover, Eulerian entropy relations are equivalent to all Lagrangian entropy relations (see [9] for further detail).

Example 2.1. For simplicity of notation, we take (t,x) as the Lagrangian coordinates. Then the system of equations

$$\begin{cases} \partial_t \tau - \partial_x u = 0, \\ \partial_t u + \partial_x p(\tau) = 0, \end{cases} \tag{79}$$

is a one-dimensional isentropic gas dynamics in Lagrangian coordinates which is also known as p-system. It is the simplest nontrivial example of a nonlinear system of conservation laws. Here τ is the specific volume, u is the velocity, and the pressure $p = p(\tau)$ is given as a function of τ by

$$p(\tau) = \kappa\tau^{-\gamma}, \quad \gamma > 0, \quad \kappa = \frac{(\gamma-1)^2}{4\gamma}. \tag{80}$$

The system (79) is equivalent to

$$\partial_t V + \partial_x f(V) = 0, \quad \text{with} \quad V = \begin{pmatrix} \tau \\ u \end{pmatrix}, \quad f(V) = \begin{pmatrix} -u \\ p(\tau) \end{pmatrix}, \tag{81}$$

where $\tau > 0$ and $(\tau, u) \in \mathbb{R}^2$. If we assume that $p'(\tau) < 0$, it follows that the Jacobian matrix of f

$$J(f) = \begin{pmatrix} 0 & -1 \\ p'(\tau) & 0 \end{pmatrix} \tag{82}$$

has two real distinct eigenvalues $\sigma_1 = -\sqrt{(-p'(\tau)} < \sigma_2 = \sqrt{-p'(\tau)}$. In other words, the system (81) is strictly hyperbolic. On the other hand, for the case $p'(\tau) > 0$, it becomes elliptic. Moreover, one can verify that the solutions of the p-system (79) and the Euler system (57) are equivalent.

3. Godunov schemes

The Godunov scheme deals with solving the Riemann problem forward in time for each grid cell and then taking the mean value over these cells. The Riemann problem is solved per mesh point at each time step iteratively. If there are no strong shock discontinuities, this process may cost much and will not be effective. To get rid of such a situation, we establish approximate Riemann solvers that are easier to implement and also low cost to use. Eulerian and Lagrangian Godunov schemes are current Godunov scheme in literature. Both have advantages and disadvantages depending on the structure of the problem. A brief comparison of the method for these two approaches is presented in the last part of the chapter. In this work we will not go further in numerical examples and details of these methods; instead, we aim to present a general form of Godunov schemes for gas dynamics in Eulerian and Lagrangian coordinate. Before introducing these, we present a first-order Godunov scheme for scalar conservation laws.

3.1 First-order Godunov scheme

Consider the scalar conservation law (1). Godunov scheme is a numerical scheme which takes advantage of analytical solutions of the Riemann problem for the conservation law (1). The numerical flux functions are evaluated at the spatial steps $x_{j-1/2}$ and $x_{j+1/2}$ by handling the solutions of the Riemann problem. On each grid cell $\mathcal{I}_i = \left[x_{j-1/2}, x_{j+1/2}\right]$, we have a piecewise constant function. The Riemann problem for (1) for the left and right sides of $\mathcal{I}_i$ are described by

$$u_L(x) = \begin{cases} u_{j-1}^n & ;x<0, \\ u_j^n & ;x>0, \end{cases} \qquad u_R(x) = \begin{cases} u_j^n & ;x<0, \\ u_{j+1}^n & ;x>0, \end{cases} \tag{83}$$

respectively. These two solutions to the Riemann problem will be the numerical solution $\tilde{u}(t,x)$. Once establishing the solution over the mesh $[t^n, t^{n+1}]$, we approximate the solution at the next time step t^{n+1} by the average value

$$U_j^{n+1} = \frac{1}{\Delta x}\int_{x_{j-1/2}}^{x_{j+1/2}} \tilde{u}\left(x, t^{n+1}\right) dx. \tag{84}$$

Proceeding this process, we define the solution $\tilde{u}(x,t^{n+1})$ iteratively. Then U_j^{n+1} can be calculated by using the integral form of the conservation law (1) in the following way: We integrate (1) for $u(t,x)$ over each grid cell $[t_n, t_{n+1}] \times I_j$:

$$\begin{aligned} &\int_{x_{j-1/2}}^{x_{j+1/2}} \tilde{u}^n\left(x, t^{n+1}\right) dx - \int_{x_{j-1/2}}^{x_{j+1/2}} \tilde{u}^n(x,t^n)\, dx \\ &\qquad = \int_{t^n}^{t^{n+1}} f\left(\tilde{u}_{j-1/2}^n\right) dt - \int_{t^n}^{t^{n+1}} f\left(\tilde{u}_{j+1/2}^n\right) dt. \end{aligned} \tag{85}$$

Dividing both parts by Δx and using the fact that $\tilde{u}(x,t^n) = u_j^n$ is constant at the end points $x_{j-1/2}$ and $x_{j+1/2}$, we get

$$u_j^{n+1} = u_j^n - \frac{\Delta t}{\Delta x}\left(f\left(\tilde{u}_{j-1/2}^n\right) - f\left(\tilde{u}_{j+1/2}^n\right)\right). \tag{86}$$

Thus, Godunov method is a conservative numerical scheme. It can be restated in an alternative form. Assigning the constant value of u_j^n at the points $x_{j-1/2}$ and $x_{j+1/2}$ by $u^*(U_{j-1}^n, U_j^n)$ and $u^*(U_j^n, U_{j+1}^n)$, respectively, the numerical flux functions become

$$\begin{aligned} f\left(\tilde{u}_{j-1/2}^n\right) &= f\left(u^*\left(U_{j-1}^n, U_j^n\right)\right) = \mathcal{F}\left(U_{j-1}^n, U_j^n\right), \\ f\left(\tilde{u}_{j+1/2}^n\right) &= f\left(u^*\left(U_j^n, U_{j+1}^n\right)\right) = \mathcal{F}\left(U_j^n, U_{j+1}^n\right). \end{aligned} \tag{87}$$

Therefore, a first-order Godunov method takes the form

$$U_j^{n+1} = U_j^n - \frac{\Delta t}{\Delta x}\left(\mathcal{F}\left(U_j^n, U_{j+1}^n\right) - \mathcal{F}\left(U_{j-1}^n, U_j^n\right)\right). \tag{88}$$

Here the constant value of $\tilde{u}n$ depends on the initial data. In other words, the Godunov method considers the Riemann problem as constant in each grid interval $\mathcal{I}_i$. It follows that, at the subsequent time stage, the exact solutions of the problem are picked as the numerical fluxes at the grid boundary.

The Godunov method is *consistent* with the exact solution of the Riemann problem for the conservation law (1). If we suppose that $u_j^n = u_j^{n+1} = \overline{u}$, then $\tilde{u}_{j+1/2}^n = \overline{u}$ and $\mathcal{F}(\overline{u},\overline{u}) = f(\overline{u})$. For the stability, CFL condition requires that

$$\sup_{x\in\mathcal{R}, t>0} |f'(u(t,x))| \frac{\Delta t}{\Delta x} \le 1 \tag{89}$$

for each u_j^n. Next, if assigning u^* as the intermediate value over the grid $\mathcal{I}_i$ in the Riemann solution, it implies that

$$u^*(u_L, u_R) = \begin{cases} u_L, & \lambda > 0, \\ u_R, & \lambda < 0, \end{cases} \tag{90}$$

where λ is the wave propagation speed. Hence the numerical flux for Godunov's method can be generalized by

$$f(u_L, u_R) = \begin{cases} \min\limits_{u_L \le u \le u_R} f(u), & \text{if} \quad u_L \le u_R, \\ \max\limits_{u_L \ge u \ge u_R} f(u), & \text{if} \quad u_R < u_L. \end{cases} \tag{91}$$

For numerical illustration of Godunov schemes, we cite the articles [14, 20, 27].

3.2 Godunov method in Eulerian coordinates

We consider Eq. (59) with (60). The eigenvalues of $F'(U)$ are $\sigma_1 = u - c < \sigma_2 = u < \sigma_3 = u + c$. Then the Riemann problem at the point $x_{i+1/2}$ between the states U_i and U_{i+1} which is solved by the Godunov scheme can be written by

$$\begin{cases} \rho_i^{n+1} = \rho_i^n - \dfrac{\Delta t}{\Delta x_i}\left((\rho u)_{i+1/2}^n - (\rho u)_{i-1/2}^n\right) \\ (\rho u)_i^{n+1} = (\rho u)_i^n - \dfrac{\Delta t}{\Delta x_i}\left(\left(\rho u^2 + p\right)_{i+1/2}^n - \left(\rho u^2 + p\right)_{i-1/2}^n\right). \\ (\rho e)_i^{n+1} = (\rho e)_i^n - \dfrac{\Delta t}{\Delta x_i}\left(((\rho e + p)u)_{i+1/2}^n - ((\rho e + p)u)_{i-1/2}^n\right) \end{cases} \tag{92}$$

3.3 Godunov method in Lagrangian coordinates

Consider the initial condition for a quantity v given by the mean value

$$v_i^0 = \frac{1}{\Delta \xi_i} \int_{\xi_{i-1/2}}^{\xi_{i+1/2}} v(\xi, 0)\, d\xi. \tag{93}$$

The eigenvalues satisfy $\sigma_1 < \sigma_2 = 0 < \sigma_3$. Setting $u_{i+1/2}$ and $p_{i+1/2}$ as the values of u and p at the contact discontinuity between V_i^n and V_{i+1}^n, it follows that

$$F\left(\left(w_R\left(0; V_i^n, V_{i+1}^n\right)\right)\right) = \left(-u_{i+j/2}^n, p_{i+j/2}^n, (pu)_{i+j/2}^n\right)^T. \tag{94}$$

Then Godunov scheme for the Lagrangian coordinates takes the form

$$\begin{cases} \tau_i^{n+1} = \tau_i^n + \dfrac{\Delta t}{\Delta m_i}\left(u_{i+1/2}^n - u_{i-1/2}^n\right) \\ u_i^{n+1} = u_i^n - \dfrac{\Delta t}{\Delta m_i}\left(p_{i+1/2}^n - p_{i-1/2}^n\right) \\ e_i^{n+1} = e_i^n - \dfrac{\Delta t}{\Delta m_i}\left((pu)_{i+1/2}^n - (pu)_{i-1/2}^n\right) \end{cases} \tag{95}$$

where

$$\Delta m_i = \rho_i^0 \Delta \xi_i, \qquad p_i^n = p\left(\tau_i^n, \varepsilon_i^n\right), \quad \varepsilon_i^n = e_i^n - \frac{\left(u_i^n\right)^2}{2}. \tag{96}$$

If we now consider the moving coordinates, Godunov scheme can also be derived equivalently by the following. Setting $x_{i+1/2} = \xi_{i+1/2}$ with the approximation of $u = dx/dt$, it follows that the Eulerian coordinate $x_{i+1/2}$ of the interface $\xi_{i+1/2}$ at t_n is upgraded with respect to

$$x_{i+1/2}^{n+1} = x_{i+1/2}^n + \Delta t u_{i+1/2}^n. \tag{97}$$

Next we deduce

$$\rho_i^n \left(x_{i+1/2}^n - x_{i-1/2}^n\right) = \Delta m_i \tag{98}$$

by a simple induction process. Hence the Lagrangian Godunov schemes become

$$\begin{cases} \Delta m_i = \rho_i^0 \left(x_{i+1/2}^0 - x_{i-1/2}^0\right) \\ x_{i+1/2}^{n+1} = x_{i+1/2}^n + \Delta t u_{i+1/2}^n \end{cases} \tag{99}$$

with

$$\begin{cases} \rho_i^{n+1} = \left(x_{i+1/2}^{n+1} - x_{i-1/2}^{n+1}\right)^{-1} \Delta m_i \\ u_i^{n+1} = u_i^n - \dfrac{\Delta t}{\Delta m_i}\left(p_{i+1/2}^n - p_{i-1/2}^n\right). \\ e_i^{n+1} = e_i^n - \dfrac{\Delta t}{\Delta m_i}\left((pu)_{i+1/2}^n - (pu)_{i-1/2}^n\right) \end{cases} \tag{100}$$

Notice that the Lagrangian Godunov schemes can be reformulated as a finite volume method. Equation (100) can be written in conservative form:

$$\partial_t(\varphi J) + \partial_\xi f = 0. \tag{101}$$

If we integrate these equations on $\left(\xi_{i-1/2}, \xi_{i-1/2}\right)$ it follows that

$$\frac{d}{dt}\int_{x_{i-1/2}}^{x_{i+1/2}} \varphi d\xi + \left(f_{i+1/2} - f_{i-1/2}\right) = 0. \tag{102}$$

Here we omit the dependency of f, φ and x on t. Moreover, if we suppose that φ is constant in each cell $\left(\xi_{i-1/2}, \xi_{i-1/2}\right)$, it follows by an explicit one-step method that is

$$\Delta x_i^{n+1} \varphi_i^{n+1} = \Delta x_i^n \varphi_i^n - \Delta t\left(f_{i+1/2}^n - f_{i-1/2}^n\right). \tag{103}$$

Moreover, if (ρ, u, e) are constant in each cell with $v = u$, we get the Godunov scheme:

$$\begin{cases} \Delta x_i^n \rho_i^n = \Delta m_i \\ \Delta m_i^{n+1} u_i^{n+1} = \Delta m_i^n u_i^n - \Delta t\left(p_{i+1/2}^n - p_{i-1/2}^n\right) \\ \Delta m_i^{n+1} e_i^{n+1} = \Delta m_i^n e_i^n - \Delta t\left((pu)_{i+1/2}^n - (pu)_{i-1/2}^n\right) \end{cases} \tag{104}$$

provided $\left(u_{i+1/2}^n, p_{i+1/2}^n\right)$ are determined by the solution of the Riemann problem, which is the desired result.

3.4 Comparison of Eulerian and Lagrangian schemes

In the literature there are two types of Godunov schemes: the Eulerian and Lagrangian. To compare one with the other, both have advantages and disadvantages. These are briefly listed in the following:

3.4.1 Eulerian approach

It is more nature; that is the properties of a flow field are described as functions of the coordinates which are in the natural physical space and time. The flow is determined by examining the behavior of the functions. Eulerian coordinates correspond to the coordinates of a fixed observer. This approach is ease of implementation and computation. The computational grids derived from the geometry constraints are generated in advance. The computational cells are fixed in space, and the fluid particles move across the cell interfaces. Since the Eulerian schemes consider the implementation at the nodes of a fixed grid, this may lead to spurious oscillations for the problems like diffusion-dominated transport equations. By adding artificial diffusion, one can get rid of these oscillations; however the nature of the problem may differ from the original one. Besides, refining the grids may also lead to remove numerical oscillations, but this process may augment the computation cost. Besides, while refining the grids, it may cause restriction of the size of time step which is limited by CFL condition. This restriction does not occur in Lagrangian case.

3.4.2 Lagrangian approach

It is based on the notion of mass coordinate denoted by $m(\xi)$. An important feature of the mass coordinate is that two segments have the same length if the mass contained in these segments is the same. This leads to face with a disadvantage; that is, at each iteration time step, the problem has to be converted from the natural coordinate system to the mass coordinate system. Once the solution at the next step is known, it has to be remapped into the natural coordinate system. As a result, this process raises the cost of the computation. Lagrangian coordinates are associated to the local flow velocity. In other words, as the velocity has different values in different parts of the fluid, then the change of coordinates is different from one point to another one in Lagrangian coordinates. Thus Lagrangian coordinates are equivalent to the Eulerian coordinates at another time. Lagrangian description states the motions and properties of the given fluid particles as they travel to different locations. Hence the computational grid points are precisely fluid particles. Since the particle paths in steady flow coincide with the streamlines, no fluid particles will cross the streamlines. Hence, there is no convective flux across cell boundaries, and the numerical diffusion is minimized. As a result, Godunov method in a Lagrangian grid is easier to handle. Moreover, in the case of higher schemes, the

subsonic character of the flow makes the transformation much easier than in Eulerian schemes. Lagrangian schemes consider the implementation in a grid that moves with the flow which is an advantage for the problems like the transport equations since the advective and diffusion terms can separately be examined.

Apart from the two main approaches, there is another method which is a combination of both, so-called Eulerian-Lagrangian methods. It combines the advantages and eliminates disadvantages of both approaches to get a more efficient method. For further details we address the reader to the reference in the next part.

Notes

We have tried to present only the theoretical aspects of scalar conservation laws with some basic models and provide some examples of computational methods for the scalar models. There are plenty of contributors to the subject; however, we just cite some important of these and the references therein. Scalar conservation laws are thoroughly studied in particular in [12]; for a more general introduction including systems, see [13, 15, 18, 19, 22] and the references therein. There are some important works related to the concept of entropy provided by [7, 15, 16]. A more precise study of the shock and rarefaction waves can be found in [23]. A simple analysis for inviscid Burgers' equation is done by [21]. The readers who are deeply interested in systems of conservation laws and the Riemann problem should see [8, 13, 15, 22, 24]. A well-ordered work of the propagation and the interaction of nonlinear waves are provided by [26]. We refer the reader to the papers [1, 17] for the theory of hyperbolic conservation laws on spacetime geometries and finite volume analysis with different aspects. A widely introductory material for finite difference and finite volume schemes to scalar conservation laws can be found in [18]. In this chapter we have studied the one-dimensional gas dynamics on the Eulerian and Lagrangian coordinates. For the detail on the Lagrangian conservation laws, we refer [10]; moreover for both Eulerian and Lagrangian conservation laws, we cite [11]. The proof of the equivalency of the Euler and Lagrangian equations for weak solutions is given in [25]. There are several numerical works for Lagrangian approach; some of the basic works on Lagrangian schemes are given in [2–6]. We refer the reader to the book [7] for a detailed analysis of the mathematical standpoint of compressible flows. Moreover Godunov-type schemes are precisely analyzed in [14, 27]; whereas, Lagrangian Godunov schemes can be found in [2, 12, 20]. As a last word, we must cite [9] as a recent and more general book consisting of scalar and system approaches of both Eulerian and Lagrangian conservation laws with theoretical and numerical parts which can be a basic source for the curious readers.

Author details

Baver Okutmuştur
Middle East Technical University, Ankara, Turkey

*Address all correspondence to: baver@metu.edu.tr

References

[1] Amorim P, LeFloch PG, Okutmustur B. Finite volume schemes on Lorentzian manifolds. Communications in Mathematical Sciences. 2008;**6**(4): 1059-1086

[2] Barlow AJ, Roe PL. A cell centred Lagrangian Godunov scheme for shock hydrodynamics. Computers and Fluids. 2011;**46**:133-136

[3] Carre G, Del Pino S, Despres B, Labourasse E. A cell-centered Lagrangian hydrodynamics scheme on general unstructured meshes in arbitrary dimension. Journal of Computational Physics. 2009;**228**: 5160-5183

[4] Cheng J, Shu CW, Zeng Q. A conservative Lagrangian scheme for solving compressible fluid flows with multiple internal energy equations. Communications in Computational Physics. 2012;**12**(5):1307-1328

[5] Clair G, Despres B, Labourasse E. A new method to introduce constraints in cell-centered Lagrangian schemes. Computer Methods in Applied Mechanics and Engineering. 2013; **261-262**:56-65

[6] Claisse A, Despres B, Labourasse E, Ledoux F. A new exceptional points method with application to cell-centered Lagrangian schemes and curved meshes. Journal of Computational Physics. 2012;**231**(11): 4324-4354

[7] Courant R, Friedrich KO. Supersonic Flow and Shock Waves. New York: Springer-Verlag, Interscience Publishers; 1948

[8] Dafermos CM. Hyperbolic Conservation Laws in Continuum Physics, Grundlehren der mathematischen Wissenschaften. Vol. 325. Berlin Heidelberg: Springer-Verlag; 2000

[9] Despres B. Numerical Methods for Eulerian and Lagrangian Conservation Laws. Birkhauser; 2017

[10] Despres B. Lagrangian systems of conservation laws. Numerische Mathematik. 2001;**89**:99-134

[11] Despres B. Lois de Conservation Euleriennes et Lagrangiennes, Mathematiques et Applications. Berlin Heidelberg: Springer-Verlag; 2009

[12] Godlevski E, Raviart PA. Numerical Approximation of Hyperbolic Systems of Conservation Laws, Applied Mathematical Sciences. Vol. 118. New York: Springer-Verlag; 1996

[13] Godlevski E, Raviart PA. Hyperbolic Systems of Conservation Laws. Paris, France: Ellipse; 1991

[14] Guinot V. Godunov–Type Schemes: An Introduction for Engineers. 1st ed. Amsterdam, Netherlands: Elsevier; 2003

[15] Lax PD. Hyperbolic systems of conservation laws and the mathematical theory of shock waves. In: Conf. Board. Math. Sci. Regional Conferences series in Applied Math., vol. 11. SIAM, Philadelphia; 1972

[16] LeFloch PG. Hyperbolic Systems of Conservation Laws: The Theory of Classical and Nonclassical Shock Waves. ETH Lecture Notes Series, Birkhauser; 2002

[17] LeFloch PG, Okutmustur B. Hyperbolic conservation laws on spacetimes. A finite volume scheme based on differential forms. Far East Journal of Mathematical Sciences. 2008; **31**:49-83

[18] LeVeque RJ. Finite Volume Methods for Hyperbolic Problems. 1st ed. Cambridge, England: Cambridge University Press; 2002

[19] Liu TP. Nonlinear stability of shock waves for viscous conservation laws. AMS Memoirs, 328, Providence; 1985

[20] Munz D. On Godunov-type schemes for Lagrangian gas dynamics. SIAM Journal on Numerical Analysis. 1994;**31**(1):17-42

[21] Oyar N. Inviscid Burgers equation and its numerical solutions [Master thesis]. Ankara, Turkey: METU; 2017

[22] Serre D. Systems of Conservation Laws 1–2. Cambridge, England: Cambridge University Press; 1999

[23] Smoller J. Shock Waves and Reaction–Diffusion Equations. New York: Springer-Verlag; 1967

[24] Toro EF. Riemann Solvers and Numerical Methods in Fluid Dynamics. A Practical Introduction. 3rd ed. Berlin Heidelberg: Springer-Verlag; 2009

[25] Wagner DH. Equivalence of the Euler and Lagrangian equations of gas dynamics for weak solutions. The Journal of Differential Equations. 1987; **68**:118-136

[26] Whitham G. Linear and Nonlinear Waves. New York: Wiley-Interscience; 1974

[27] Van Leer B. On the relation between the upwind-differencing schemes of Godunov, Engquist-Osher and Roe. SIAM Journal on Scientific and Statistical Computing. 2012;**5**:1-20